View Article Online / Journal Homepage / Table of Contents for this issue

Molecular, electronic structure and spectroscopic properties of MM quadruply bonded units supported by *trans*-6-carboethoxy-2-carboxylatoazulene ligands†

Brian G. Alberding,[a] Mikhail V. Barybin,*[b] Malcolm H. Chisholm,*[a] Terry L. Gustafson,*[a] Carly R. Reed,[a] Randall E. Robinson,[b] Nathan J. Patmore,[a] Namrata Singh[a] and Claudia Turro*[a]

Received 16th September 2009, Accepted 24th November 2009
First published as an Advance Article on the web 13th January 2010
DOI: 10.1039/b919282d

Published on 13 January 2010. Downloaded by Ludwig Maximilians Universitaet Muenchen on 20/06/2014 09:49:00.

The reaction between $M_2(TiPB)_4$ (M = Mo, W) where TiPB = 2,4,6-triisopropylbenzoate and 6-carboethoxy-2-azulenecarboxylic acid (2 equiv.) in toluene leads to the formation of complexes $M_2(TiPB)_2$(6-carboethoxy-2-azulenecarboxylate)$_2$. Compound **I** (M = Mo) is blue and compound **II** (M = W) is green. Both are air sensitive, hydrocarbon soluble species that gave the corresponding molecular ions in their mass spectra (MALDI-TOF). They show metal based oxidations and ligand based reductions. Electronic structure calculations (DFT and time dependent DFT) indicate that the two azulene carboxylate π systems are coupled by their interactions with the M_2 δ orbitals. Their intense colors arise from M_2 δ to azulene π* electronic transitions. While compound **I** exhibits weak emission at ~ 900 nm, no emission has been detected for **II**. Both **I** and **II** have been studied by fs and ns transient absorption spectroscopy. The X-ray analysis of the molecular structure of **II** in the solid state confirmed the paddlewheel nature of its $W_2(O_2C)_4$ core and the *trans* orientation of the ligands.

Introduction

We have for some time been studying the properties of linked MM quadruply bonded complexes (M = Mo or W) where the linker is a dicarboxylate or a related unit capable of electronically coupling the two M_2 units by way of M_2 δ to bridge π conjugation.[1-3] The key orbital interactions are shown in **A** below. The out-of-phase combination of the M_2 δ orbitals finds a symmetry match with filled π orbitals involving the CO_2 fragments and the in-phase combination of the M_2 δ orbitals interacts with the π* orbital involving the CO_2 junctions.

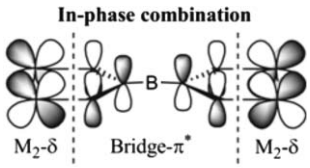

A

Of these two orbital interactions, the back bonding, M_2 (δ) to CO_2 (π*) interaction is more important based on relative orbital energies and this interaction is stronger for M = W than for M = Mo. Single electron oxidation of such linked dinuclear compounds leads to metal based mixed valence species that have interesting spectroscopic properties and can traverse the class II/III border.[4,5] We recognized that the M_2 center might also accommodate mixed valence ligands in a *trans* oriented molecule upon reduction. Here the key orbital interaction is shown in B below where the out-of-phase π* ligand-based orbital interacts with the M_2 δ orbital.

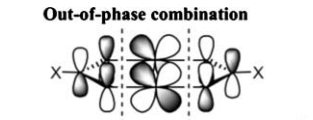

B

The two mixed valence systems described by frameworks A and B are complementary: oxidation in A and reduction in B generate metal centered and ligand centered mixed valence states, respectively. Based on our earlier studies of azulene-2,6-dicarboxylate bridged compounds,[6] we decided to use the 6-carboethoxy-2-azulene carboxylate ligand in this work. A preliminary communication of some aspect of this work has been published.[7]

Results and discussion

Syntheses

The complexes $M_2(TiPB)_4$,[8,9] (M = Mo, W), where TiPB = 2,4,6-triisopropyl benzoate were allowed to react with 6-carboethoxy-2-azulene carboxylic acid (2 equiv.) in toluene at room temperature under an Ar atmosphere. The $M_2(TiPB)_4$ compounds are yellow (M = Mo) and orange (M = W) and the substitution of the azulene carboxylate for TiPB was accompanied by a dramatic

[a]*Department of Chemistry, The Ohio State University, 100 W. 18th Avenue, Columbus, Ohio 43210*
[b]*Department of Chemistry, The University of Kansas, 1251 Wescoe Hall Drive, Lawrence, Kansas 66045-7582*

† Electronic supplementary information (ESI) available: Transient absorption spectra (fs and ns), absorption, emission and excitation spectra for the azulene carboxylic acid; DVP for the reduction of II]. See DOI: 10.1039/b919282d

View Article Online

Published on 13 January 2010. Downloaded by Ludwig Maximilians Universitaet Muenchen on 20/06/2014 09:49:00.

color change. The reactions were allowed to proceed at room temperature for 3 days yielding finely divided microcrystalline products of the title compounds **I** (M = Mo) and **II** (M = W) which were blue and pale green, respectively. The *trans* substitution is favored by the presence of the two bulky TiPB ligands as well as by M_2 (δ) to azulene carboxylate (π^*) back bonding. Compounds **I** and **II** show molecular ions $\mathbf{I}^+$ and $\mathbf{II}^+$ by MALDI-TOF mass spectrometry and their ^{1}H NMR spectra are consistent with expectations.

Molecular structure of II

A single crystal X-ray diffraction study of **II** confirmed the *trans* substitution pattern. The molecular structure of **II** is illustrated in Fig. 1. The W–W distance of 2.208 Å is typical of a W–W quadruple bond and the W–O distances 2.03 Å are as expected for a $W_2(O_2C)_4$ paddlewheel core.[10] Of particular note are the interplanar angles between the azulenyl groups and the corresponding carboxylate junctions which are 3 and 5°. As can be seen from Fig. 1, this co-planarity facilitates the extended Lπ-M_2δ-Lπ conjugation as predicted for the framework **B**. In contrast the dihedral angle involving the TiPB aromatic C-6 rings and their carboxylate junctions are 80 and 82°. This geometry allows relief of steric pressure at the dinuclear center but removes the benzoid rings from conjugation with the M_2 center. The full structural analysis of **II** was addressed in the earlier communication.[7] While we have not examined the molybdenum complex **I** crystallographically, it is reasonable to expect that **I** is structurally related to **II**.

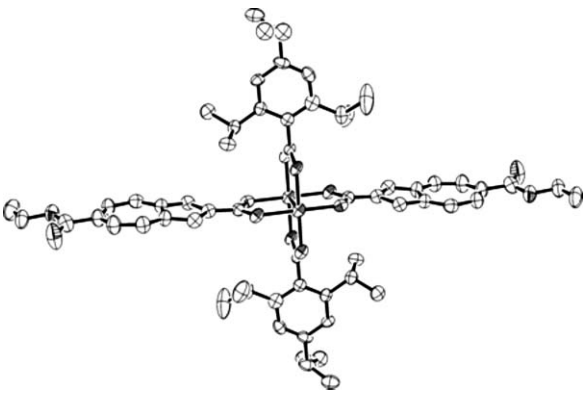

Fig. 1 Molecular structure of **II** in the solid-state. Thermal ellipsoids are drawn at the 50% probability level.

Electronic structure calculations

Electronic structure calculations were carried out on the model compounds **I′** and **II′** featuring formate ligands in place of the two *trans* TiPB groups. Given the lack of M_2 (δ) to TiPB arene (π) conjugation, the substitution of formate for TiPB was reasonable for saving computational time and resources. Calculations employed the Gaussian03 package as described in the experimental section.

A frontier orbital energy diagram comparing **I′** and **II′** is shown in Fig. 2. For both metals the HOMO is principally the M_2 δ with some ligand contribution due to back bonding. The tungsten δ orbital in **II′** is notably higher in energy than its molybdenum counterpart in **I′** as has been seen in related compounds.[1] The LUMO and LUMO+1 are the in-phase and out-of-phase combinations of an azulenecarboxylate π* orbital as expected based on the simple orbital interaction diagram **B**. The magnitude of the splitting of these two orbitals is a relative measure of the extent of back bonding and mixing with the M_2 δ orbital. Fig. 2 shows the splitting. This is greater for **II′** than for **I′** which is consistent with the relative orbital energies and overlap with the M_2 δ orbitals: W_2 > Mo_2. In both **I′** and **II′** the HOMO-1 and HOMO-2 are isoenergetic and are the in-phase and out-of-phase combinations of the azulene filled π orbitals of highest energy. These do not mix with the MM based orbitals. For the molybdenum complex these azulene π orbitals are much closer in energy (~ 0.5 eV) to the HOMO in comparison to the tungsten complex (~ 0.9 eV). The M_2 π and σ orbitals are located below the HOMO-2.

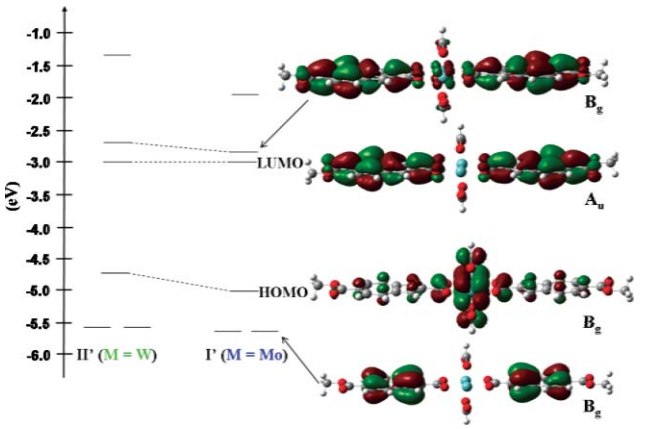

Fig. 2 Frontier orbital energy diagram comparing **I′** and **II″**. Gauss view plots for molecular orbitals of **I′** are also shown.

Electrochemical studies

The compounds **I** and **II** have been studied by cyclic voltammetry and differential pulse voltammetry in THF solution. Both complexes show reversible oxidation waves consistent with the expectation of removal of an electron from the M_2 δ orbital: **I**, 60 mV and **II**, -465 mV *versus* $Cp_2Fe^{0/+}$. The compounds also show partially reversible reduction waves that we assign to reduction of azulene carboxylate units. The DPV pattern for compound **I** is given in Fig. 3. It seems that these are both two electron reduction waves and that the first wave shows evidence of a splitting quite possibly because of the coupling of the two azulene carboxylate units *via* the Mo_2 δ orbital as predicted by the calculations. The reduction waves for **II** were more complicated and are shown in the supporting information.† Given the expected greater coupling between the azulene carboxylate π* orbitals in the tungsten compound, it is possible that each reduction wave is split into two for **II**. Unfortunately, reduction of both Mo and W systems lead to species that are kinetically labile towards decomposition.

Electronic absorption spectra

The electronic absorption spectra of **I** and **II** in THF solution are compared in Fig. 4. The lowest energy absorptions are assigned to

 This journal is © The Royal Society of Chemistry 2010

View Article Online

Published on 13 January 2010. Downloaded by Ludwig Maximilians Universitaet Muenchen on 20/06/2014 09:49:00.

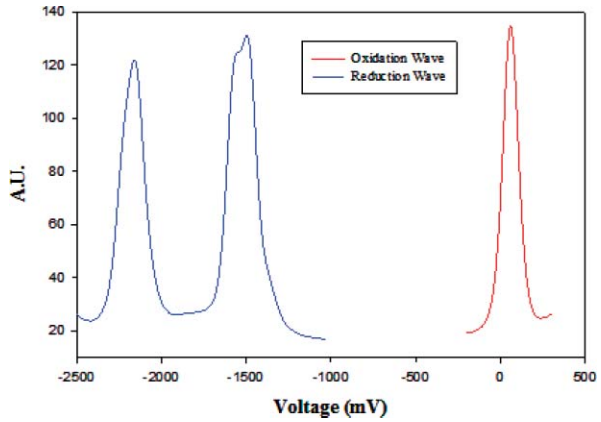

Fig. 3 DPV voltammogram exhibiting the oxidation and reduction waves for **I**.

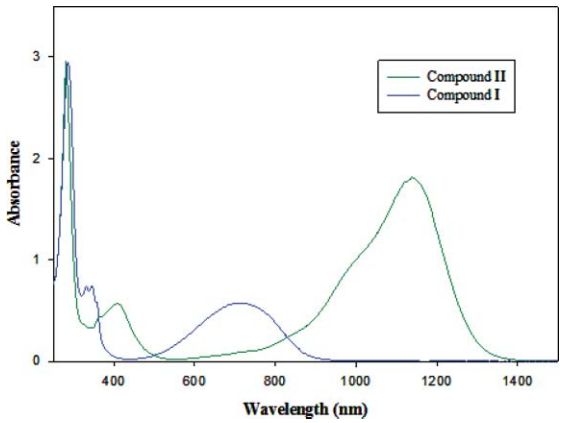

Fig. 4 Electronic absorption spectra for **I** and **II**.

^{1}MLCT involving the fully allowed HOMO to LUMO transition. The molybdenum complex shows a broad absorption with a λ_{max} at 715 nm while the tungsten complex has a sharper and even more intense absorption in the NIR at 1130 nm. In both cases the absorptions occur to lower energy relative to the calculated energies obtained by time dependent DFT. This is likely due to the fact that the calculations consider model compounds and constitute gas phase predictions. The THF solvent undoubtedly plays a role in stabilizing the photoexcited state that places positive charge on the metals. In addition, in the case of tungsten we have previously noted that the energies of ^{1}MLCT transitions are overestimated in relation to their molybdenum analogues due to the greater importance of spin–orbit coupling for the heavier 5d element.[11,12]

Time dependent calculations performed on **I′** and **II′** show that for both compounds the lowest energy electronic transition is the HOMO–LUMO transition. The calculated absorption bands and their assignments for compound **I′** and **II′** are given in Tables 1 and 2 respectively.

The HOMO to LUMO transition is a fully allowed ^{1}MLCT with very high calculated oscillator strength: $f = 1.17$ for **II′** and 0.86 for **I′**. At higher energies the TD-DFT calculations predict weaker electronic transitions involving variously mixed Lπ/Mδ/Lπ to Lπ* orbital states. For **II′** the DFT predicts a M_2 δ to TiPB CO_2 π* transition at 347 nm with $f = 0.13$. This is consistent with the observed spectrum shown in Fig. 4.

Table 1 Calculated electronic transitions and their assignments for **I′**

Wavelength/nm	Oscillator strength (f)	Assignment
672	0.858	M_2 δ to ligand π* (HOMO to LUMO)
632	0.018	Ligand π to π* (HOMO – 2 to LUMO + 1; HOMO – 1 to LUMO)
381	0.011	Ligand π to M_2 δ* (HOMO – 1 to LUMO + 2)
366	0.009	M_2 δ to ligand π* (HOMO to LUMO + 4)
350	0.201	Ligand π to π* (HOMO – 6 to LUMO; HOMO – 4 to LUMO + 1; HOMO – 2 to LUMO + 3; HOMO – 1 to LUMO + 4)

Table 2 Calculated electronic transitions and their assignments for **II′**

Wavelength/nm	Oscillator strength (f)	Assignment
779	1.170	M_2 δ to ligand π* (HOMO to LUMO)
636	0.017	Ligand π to π* (HOMO – 2 to LUMO + 1; HOMO – 1 to LUMO)
403	0.009	M_2 δ to ligand π* + M_2 δ* (HOMO to LUMO + 2; HOMO to LUMO + 4)
358	0.500	M_2 δ to ligand π* (HOMO to LUMO + 6) Ligand π to π* (HOMO – 6 to LUMO; HOMO – 5 to LUMO + 1)
347	0.135	M_2 δ to TiPB -CO_2 (HOMO to LUMO + 7)

Steady state emission spectra

Excitation of **I** in THF, into the ^{1}MLCT transition at 785 nm, results in a weak emission at room temperature in the near IR. At low temperature in 2-methyl THF, the intensity of this emission is significantly enhanced and is shown in Fig. 5.

The emission centered at 900 nm is relatively featureless and is tentatively assigned to the fluorescence from the S_1 state, ^{1}MLCT. The Stoke's shift of ~ 2800 cm^{-1} is quite large and likely reflects the change to a rigorously planar arrangement of the O_2C-azulene-CO_2 framework in the excited state, S_1. For comparison, a Stokes shift of 5300 cm^{-1} was observed for $Mo_2(TiPB)_2(O_2C\text{-terthienyl})_2$ where in the photoexcited state a planar quinoidal geometry is expected.[13] Fig. 5 illustrates that the emission tails significantly to lower energy and it is possible that this represents vibronic features associated with ν (CO_2) and ν (CC) of the azulene carboxylate that are not well resolved. In somewhat related systems of formula $Mo_2(TiPB)_2(O_2CTh_n)_2$, where Th = thienyl and $n = 1$, 2 or 3, we have observed emission from a T_1 state that is assigned to MMδδ* at 1100 nm.[13] However, in these compounds the triplet MMδδ* emissions show well resolved vibronic features arising from ν (MM). This is clearly not the case for compound **I**.

We have not been able to detect any emission from solutions of **II** which is not surprising in view of the compound's low energy ^{1}MLCT. The energy gap law would predict a fast non-radiative process to be likely.[14]

View Article Online

Published on 13 January 2010. Downloaded by Ludwig Maximilians Universitaet Muenchen on 20/06/2014 09:49:00.

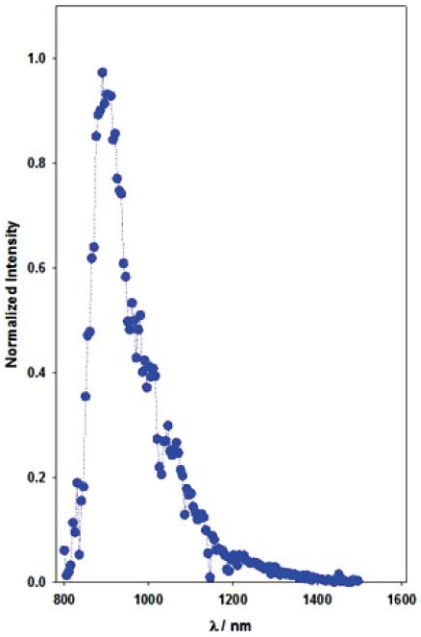

Fig. 5 Steady state emission for **I** at 77 K in 2-methyl-THF (λ_{exc} = 785 nm).

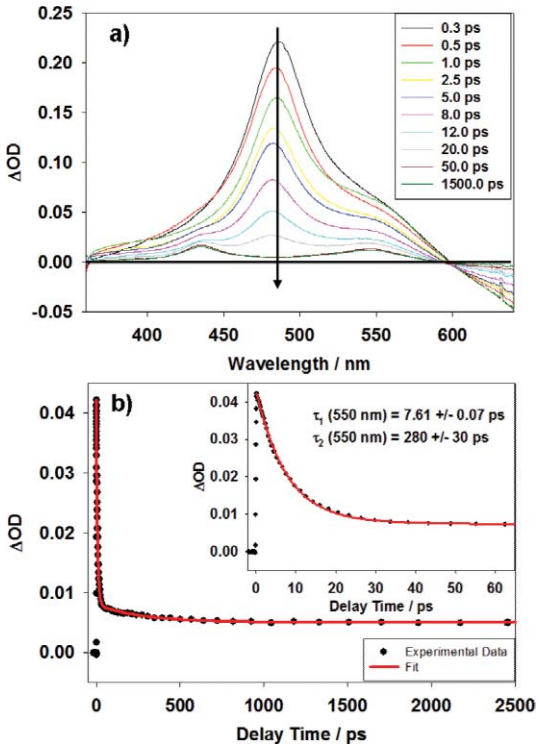

Fig. 6 a) Femtosecond broadband transient absorption spectra for **I** in THF excited at 675 nm. b) Representative single wavelength kinetics monitored at 550 nm. Inset: Early time dynamics.

Transient absorption spectroscopy

Both **I** and **II** have been studied by fs and ns transient absorption spectroscopy and short lived and long lived excited states have been observed. Compound **I** shows a transient absorption at ~ 485 nm upon irradiation at 675 nm (which is into the ^{1}MLCT). Monitoring the kinetics at 550 nm indicates that the aforementioned band decays in 7.61 ps to give rise to the triplet state absorption, indicated by the bands with maxima at 434 nm and 543 nm. Furthermore, a slower decay component with a lifetime of ~ 280 ps is observed which is attributable to vibrational cooling of the triplet state. The spectra and kinetic plots are shown in Fig. 6.

The kinetics of the triplet state for **I** have been monitored by ns transient absorption spectroscopy. Upon excitation at 532 nm the lifetime of T_1 is ~ 260 ns. This is notably shorter than the T_1 states that we have assigned to MMδδ* which typically have τ ~ 50 to 100 μs for M = Mo.[13] If our assignment of the emission at 900 nm to the S_1 state is correct, then it is likely that the ^{3}MLCT state occurs at lower energy than the ^{3}MMδδ* and decays faster by non-radiative processes due to a combination of the energy gap law and vibronic coupling with ν (CH) and ν (CC) modes. Compound **II**, when excited at 365 nm in THF, has a short lived excited state, τ = 4.5 ps with a broad absorption band at 470 nm, and then decays to the triplet state. The absorption features for T_1 are, for both compounds (see Supporting Information), similar to the absorption of the azulene radical anion[15] but for **II** the lifetime is notably shorter than that for **I**. For **II** we can only estimate it to be between 3 and 20 ns because of instrument limitations. We can reliably assign this state to ^{3}MLCT by comparison with the spectrum for reduced azulene and since its lifetime is much shorter than the ^{3}MMδδ* states that we have previously detected.[13] Moreover its energy would likely be on the order of 5000 cm^{-1}, given that the S_1 state may be estimated to be ~ 7000 cm^{-1} based on the observed ^{1}MLCT at ~ 9000 cm^{-1}. The above photophysical studies can be summarized in the form of a Jablonski diagram as shown in Fig. 7.

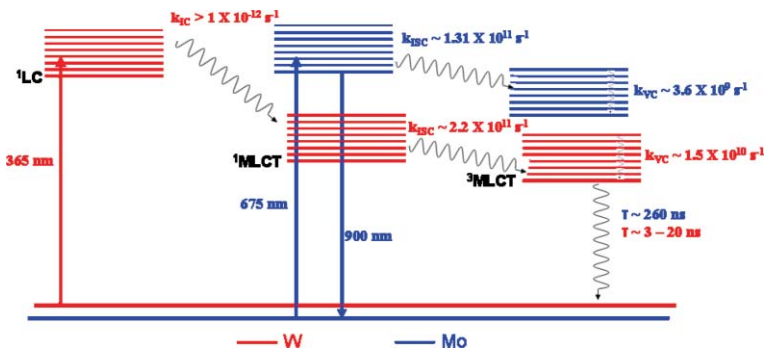

Fig. 7 Jablonski diagram summarizing observed photophysical properties of **I** (blue) and **II** (red) in THF solution.

 This journal is © The Royal Society of Chemistry 2010

View Article Online

Published on 13 January 2010. Downloaded by Ludwig Maximilians Universitaet Muenchen on 20/06/2014 09:49:00.

Conclusions

The compounds **I** and **II** exhibit interesting spectroscopic and electrochemical properties. The molybdenum complex **I** does not show any phosphorescence from the ^{3}MMδδ* state which leads us to believe that the ^{3}MLCT state lies lower in energy. This is in contrast to other compounds of the form *trans*-$Mo_2(TiPB)_2(O_2CL)$ where L = a π-conjugated ligand. The tungsten complex **II** is also unusual as it gives a low energy intense absorption in the NIR at 1130 nm. The singly reduced species $\mathbf{I}^-$ and $\mathbf{II}^-$ are proved to be kinetically labile which has hindered our characterization of these systems featuring mixed valence ligands.[16]

Experimental

General considerations

$W_2(TiPB)_2$(6-carboethoxy-2-azulenecarboxylate)$_2$, **II**, was obtained according to published procedures.[7] All manipulations were performed in a nitrogen-filled glovebox or by using standard Schlenk-line techniques. Solvents were dried using standard procedures and degassed prior to use. ^{1}H NMR spectra were recorded on a 400 MHz Bruker DPX Avance spectrometer and referenced to residual protio signals. Matrix assisted laser desorption ionization time-of-flight (MALDI-TOF) mass spectra were obtained on a Bruker Microflex mass spectrometer provided by a grant from the Ohio BioProducts Innovation Center. The spectrometer was operated in a reflective, positive ion mode. Laser power was used at the threshold level required to generate signal. The accelerating voltage was set to 28 kV. Dithranol was used as the matrix and prepared as a saturated solution in THF. Microanalysis was performed by H. Kolbe Microanalytical Laboratory. UV-Vis spectra were recorded using a Perkin Elmer Lambda 900 UV-Vis spectrometer.

Electrochemistry

Cyclic voltammograms and differential pulse voltammograms were collected using a Princeton Applied Research (PAR) 173A potentiostat-galvanostat equipped with a PAR 176 current-to-voltage converter. Electrochemical measurements were performed under an inert atmosphere in a 0.1 M solution of $Bu^n_4NPF_6$ in THF inside a single compartment voltammetric cell equipped with a platinum working electrode, a platinum wire auxiliary electrode, and a pseudo-reference electrode consisting of a silver wire in 0.1 M $Bu^n_4NPF_6$/THF separated from the bulk solution by a Vycor tip. The potentials are referenced internally to the $FeCp_2/FeCp_2^+$ couple by addition of a small amount of $FeCp_2$ to the solutions of the complexes.

Photophysical measurements

The steady-state NIR-luminescence measurements at room temperature were carried out in 1 × 1 cm square quartz cuvettes equipped with Kontes stopcocks and the measurements at 77 K were carried out in J. Young NMR tubes using an optical dewar sample holder. The spectra were measured on a home-built instrument utilizing a germanium detector. The samples were excited at 405 nm or 785 nm (laser diode max power: 45.0 mW). A RG830 long pass filter was placed between the sample and the detector.

Nanosecond transient absorption measurements were carried out in 1 × 1 cm square quartz cuvettes equipped with Kontes stopcocks on a home-built instrument pumped by a frequency doubled (532 nm) or tripled (355 nm) Spectra-Physics GCR-150 Nd:YAG laser (fwhm ~ 8ns, ~ 5 mJ per pulse). The signal from the photomultiplier tube (Hamamatsu R928) was processed by a Tektronics 400 MHz oscilloscope (TDS 380).[17]

The broadband femptosecond transient absorption experiments for $Mo_2(TiPB)_2(Azu)_2$ and $W_2(TiPB)_2(Azu)_2$ were carried out using laser and detection systems that which have been previously described.[18] The samples were excited at 675 nm for $Mo_2(TiPB)_2(Azu)_2$ and 365 nm for $W_2(TiPB)_2(Azu)_2$ (with excitation power ~ 1–2 μJ at the sample) and were prepared with absorbance ~ 0.4–0.8 at the excitation wavelength. During the measurements, the samples were kept in constant motion by manual movement of an XYZ stage in the vertical and horizontal directions. In order to ensure that no photodecomposition occurred during data collection, absorption spectra were recorded before and after the transient absorption measurements. The measurements were repeated four times at each of the pump–probe delay positions to confirm data reproducibility throughout the experiment and the resulting spectra were corrected for the chirp in the white-light super continuum.[19]

Kinetics were monitored using single probe wavelengths. In these cases, the white-light continuum was generated from a water cell having a 1 cm path length and the probe wavelengths were isolated by a 10 nm bandwidth interference filter placed between the sample and detector. The detector was a joule meter (molectron) and the signals were acquired by a lock-in amplifier (Stanford Research Systems) referenced to an optical chopper in the pump pulse path. The kinetics were fit to an exponential decay of the form, $S(t) = \sum_n a_n \exp(-t/\tau_n) + y_0$, with amplitude, a, lifetime, τ, and offset, y_0, using Origin 6.0. Error bars are reported as the standard error of the exponential fit.

Electronic structure calculations

The geometries of all the model compounds were optimized in the gas-phase using density functional theory with the aid of the Gaussian03 suite of programs. The B3LYP functional was used along with the SDD energy consistent pseudopotentials for the heavier elements, namely Mo and W, and the 6-31G* basis set for C, H, and O. Optimizations were confirmed to be a minima on the potential energy surface using harmonic vibrational frequency analysis. Orbital analyses were performed using GaussView. All orbital diagrams are shown at an isosurface value of 0.02.

Syntheses

$Mo_2(TiPB)_2$(6-carboethoxy-2-azulenecarboxylate)$_2$, I. A Schlenk tube was charged with $Mo_2(O_2C$-2,4,6-isopropyl-$C_6H_2)_4$ (0.106 g, 0.09 mmol) and 6-carboethoxy-2-azulenecarboxylic acid (0.04 g, 0.18 mmol), to which 10 mL of toluene was added. The suspension was stirred for 4 days, during which time a blue precipitate was formed. The precipitate was isolated by centrifugation and washed with 2 × 10 mL of toluene followed by 10 mL aliquot of hexane, before drying *in vacuo* to yield a blue

View Article Online

Published on 13 January 2010. Downloaded by Ludwig Maximilians Universitaet Muenchen on 20/06/2014 09:49:00.

solid. Yield: 0.08 g, 76%. Anal. Calculated for $Mo_2C_{60}H_{68}O_{12}$: C, 61.43; H, 5.84. Found: C, 58.37; H, 6.04%. UV-Vis (λ_{max}, values of $\varepsilon \times 10^{-3}$ in parentheses): 715 (7627 $M^{-1}cm^{-1}$) nm. ^1H NMR (400 MHz; THF-d_8): δ 0.9 (d, 24H), 1.2 (d, 6H), 1.4 (t, 6H), 2.8 (m, 4H), 3.5 (m, 2H), 4.4 (q, 4H), 6.9 (s, 4H), 8.1 (s, 4H), 8.2 (d, 4H), 8.6 (d, 4H). MALDI-TOF: 1173.0 (100%, M^+).

Acknowledgements

We thank the National Science Foundation and The Ohio State University for financial support and the Ohio Super Computer Center for computational resources.

References

1 M. H. Chisholm and N. J. Patmore, *Acc. Chem. Res.*, 2007, **40**, 19.
2 M. H. Chisholm and N. J. Patmore, *Chem. Rec.*, 2005, **5**, 308.
3 M. H. Chisholm and N. J. Patmore, *Dalton Trans.*, 2006, 3164.
4 B. S. Brunschwig, C. Creutz and N. Sutin, *Chem. Soc. Rev.*, 2002, **31**, 168.
5 S. F. Nelson, *Chem.–Eur. J.*, 2000, **6**, 581.
6 M. V. Barybin, M. H. Chisholm, N. S. Dalal, T. H. Holovics, N. J. Patmore, R. E. Robinson and D. J. Zipse, *J. Am. Chem. Soc.*, 2005, **127**, 15182.
7 M. V. Barybin, M. H. Chisholm, N. J. Patmore, R. E. Robinson and N. Singh, *Chem. Commun.*, 2007, 3652.
8 F. A. Cotton, L. M. Daniels, E. A. Hillard and C. A. Murillo, *Inorg. Chem.*, 2002, **41**, 1639.
9 D. J. Santure, J. C. Huffman and A. P. Sattelberger, *Inorg. Chem.*, 1985, **24**, 371.
10 *Multiple Bonds Between Metal Atoms*, *Third Edition*, ed. F. A. Cotton, C. A. Murillo and R. A. Walton, 2005.
11 M. H. Chisholm, P.-T. Chou, Y.-H. Chou, Y. Ghosh, T. L. Gustafson and M.-L. Ho, *Inorg. Chem.*, 2008, **47**, 3415.
12 B. E. Bursten, M. H. Chisholm, R. J. H. Clark, S. Firth, C. M. Hadad, A. M. MacIntosh, P. J. Wilson, P. M. Woodward and J. M. Zaleski, *J. Am. Chem. Soc.*, 2002, **124**, 3050.
13 G. T. Burdzinski, M. H. Chisholm, P. T. Chou, Y. H. Chou, F. Feil, J. C. Gallucci, Y. Ghosh, T. L. Gustafson, M. L. Ho, Y. Liu, R. Ramnauth and C. Turro, *Proc. Natl. Acad. Sci. U. S. A.*, 2008, **105**, 15247.
14 R. Englman and J. Jortner, *Mol. Phys.*, 1970, **18**, 145.
15 T. Shide, *Electronic, Absorption Spectra of Radical Ions*, Elsevier, Amsterdam, 1988, Vol. Physical Sciences data 34.
16 P. H. Dinolfo and J. T. Hupp, *J. Am. Chem. Soc.*, 2004, **126**, 16814.
17 M. J. Byrnes, M. H. Chisholm, J. C. Gallucci, Y. A. Liu, R. Ramkrishna and C. Turro, *J. Am. Chem. Soc.*, 2005, **127**, 17343.
18 G. Burdzinski, J. C. Hackett, J. Wang, T. L. Gustafson, C. M. Hadad and M. S. Platz, *J. Am. Chem. Soc.*, 2006, **128**, 13402.
19 T. Nakayama, Y. Amijima, K. Ibuki and K. Hamanoue, *Rev. Sci. Instrum.*, 1997, **68**, 4364.

 This journal is © The Royal Society of Chemistry 2010